0013-7227/05/$15.00/0
Printed in U.S.A.

Endocrinology 146(2):655–665

doi: 10.1210/en.2004-0766

Skeletal Overexpression of Gremlin Impairs Bone Formation and Causes Osteopenia

Elisabetta Gazzerro, Renata C. Pereira, Vanda Jorgetti, Sarah Olson, Aris N. Economides, and Ernesto Canalis

Department of Research (E.G., R.C.P., S.O., E.C.), Saint Francis Hospital and Medical Center, Hartford, Connecticut 06105-1299; Department of Medicine, University of Connecticut School of Medicine (E.G., R.C.P., E.C.), Farmington, Connecticut 06030; Regeneron Pharmaceuticals, Inc. (A.N.E.), Tarrytown, New York 10591; and Laboratorio de Fisiopatologia Renal (V.J.), Universidade de Sao Paulo, Sao Paulo, Brazil

Skeletal cells synthesize bone morphogenetic proteins (BMPs) and BMP antagonists. Gremlin, a BMP antagonist, is expressed in osteoblasts and opposes BMP effects on osteoblastic differentiation and function *in vitro*. However, its effects *in vivo* are not known. To investigate the actions of gremlin on bone remodeling *in vivo*, we generated transgenic mice overexpressing gremlin under the control of the osteocalcin promoter. Gremlin transgenics exhibited bone fractures and reduced bone mineral density by 20–30%, compared with controls. Static and dynamic histomorphometry of femurs revealed that gremlin overexpression caused reduced trabecular bone volume and the appearance of woven bone. Polarized light microscopy revealed disorganized collagen bundles at the endosteal cortical surface. Gremlin transgenic mice displayed a 70% decrease in the number of osteoblasts/trabecular area and reduced mineral apposition and bone formation rates. *In vivo* bromodeoxyuridine labeling and marrow stromal cell cultures demonstrated an inhibitory effect of gremlin on osteoblastic cell replication, but no change on apoptosis was detected. Marrow stromal cells from gremlin transgenics displayed a reduced response to BMP on phosphorylated mothers against decapentaplegic 1/5/8 phosphorylation and reduced free cytosolic β-catenin levels. In conclusion, transgenic mice overexpressing gremlin in the bone microenvironment have decreased osteoblast number and function leading to osteopenia and spontaneous fractures. (*Endocrinology* 146: 655–665, 2005)

SKELETAL CELLS SYNTHESIZE a number of growth factors including bone morphogenetic proteins (BMPs), which play a critical role in skeletal development and the maintenance of bone homeostasis (1). BMPs are unique because they induce the differentiation of mesenchymal cells toward the osteoblastic lineage and enhance the function of the osteoblast, playing an autocrine role in osteoblast formation and function. However, BMP activities are tempered by intracellular and extracellular antagonists, and their importance is documented by experimental studies and genetic human disorders (2–6). Extracellular BMP antagonists are a group of secreted proteins, which include noggin, the chordin family, members of the differentially screening-selected gene aberrative in neuroblastoma (DAN)/Cerberus family, and twisted gastrulation (7–11). These antagonists bind to their cognate BMPs, preventing their binding to their signaling receptors, although activities independent of BMP binding have been suggested. Each extracellular antagonist binds specific members of the BMP superfamily with different affinity.

First Published Online November 11, 2004

Abbreviations: BFR, Bone formation rate; BMC, bone mineral content; BMD, bone mineral density; BMP, bone morphogenetic protein; BrdU, bromodeoxyuridine; DAN, differentially screening-selected gene aberrative in neuroblastoma; *drm*, down-regulated by v-mos; FBS, fetal bovine serum; Smad, phosphorylated mothers against decapentaplegic; TBS, Tris-buffered saline.

***Endocrinology* is published monthly by The Endocrine Society (http://www.endo-society.org), the foremost professional society serving the endocrine community.**

Gremlin, a highly conserved 20.7-kDa glycoprotein, is a member of the DAN/Cerberus family and was originally isolated in *Xenopus* embryos as an anti-BMP dorsalizing agent (12). Gremlin and its rat homolog, *drm* (down-regulated by v-mos), are secreted glycoproteins and are present in the extracellular matrix but also are found in the endoplasmic reticulum (13). Gremlin/*drm* binds and prevents the activity of BMP-2, -4, -7. Its synthesis is reduced in neoplastic cells, and it is considered to play a negative role on cell survival acting as a tumor suppressor gene (14). Homozygous null mutations of the gremlin gene in mice result in serious developmental limb abnormalities and lethality. Nullizygous embryos and newborns display only one bone in the zeugopod, the median segment of the developing limb of both fore- and hindlimbs, fewer digits, and abnormal maintenance of interdigital tissue (15). The patterning of distal limb skeletal elements is tightly regulated by the reciprocal interactions between BMPs, fibroblast growth factor 4, and Sonic Hedgehog. Gremlin is secreted in the limb bud, and by inhibiting the action of local BMPs, it enhances fibroblast growth factor 4 activity and promotes proximodistal limb outgrowth and development (16, 17).

The role of gremlin in the adult skeleton is unknown. Osteoblasts express gremlin, which is increased after BMP exposure, suggesting the presence of local feedback mechanisms to regulate BMP activity by gremlin (18). *In vitro*, gremlin decreases the stimulatory effects of BMP on osteoblastic function. Previous work from our laboratory has described that transgenic mice overexpressing the BMP antagonist noggin exhibit severe osteopenia and profound inhibition

of bone formation (19). Although noggin and gremlin bind and prevent BMP functions *in vitro*, independent activities have not been excluded. It is possible that noggin and gremlin act in a complementary fashion and not as redundant signals. The consequences of gremlin overexpression in adult skeletal tissue *in vivo* are not known. Therefore, this study assessed the direct effects of gremlin on bone remodeling. For this purpose, we created transgenic mice overexpressing gremlin under the control of the osteoblastic specific osteocalcin promoter and determined their skeletal phenotype.

Materials and Methods

Osteocalcin/gremlin construct

After introduction of the Kozak consensus sequence upstream of the translation initiation codon, the 0.56-kb fragment coding human gremlin was cloned downstream of a 1.7-kb fragment of the rat osteocalcin promoter (Dr. R. Derynck, University of California, San Francisco, CA) (20). The second intron of the rabbit β-globin gene (0.6 kb) was included between the osteocalcin promoter and gremlin coding sequences, which were followed by a 0.2 kb-fragment containing polyadenylation sequences from the bovine GH gene. Nucleotide sequence analysis confirmed the absence of mutations and the correct orientation of the construct. The ability of the construct to direct gremlin expression *in vitro* was confirmed by transiently transfecting the transgene construct into ROS17/2 osteosarcoma cells, identification of gremlin transgene by Northern blot analysis, and protein by Western blot analysis (not shown).

Generation of transgenic mice

Microinjection of linearized DNA into pronuclei of fertilized oocytes from CD-1 outbred albino mice (Charles River Laboratories, Cambridge, MA), and transfer of microinjected embryos into pseudopregnant mice were carried out by the transgenic facility at the University of Connecticut Health Center. Positive founders were identified by Southern blot analysis of tail DNA. Genomic DNA was digested with the restriction endonuclease, *Bam*HI, resolved by electrophoresis on a 0.8% Seakem LE agarose gel (Cambrex Bio Science, Rockland, ME), blotted onto GeneScreen Plus charged nylon (PerkinElmer, Norwalk, CT), hybridized with a 0.6-kb human gremlin cDNA (Regeneron Pharmaceuticals Inc., Tarrytown, NY), and washed as previously described (19, 21). The bound radioactive material was visualized by autoradiography on X-AR5 film (Eastman Kodak, Rochester, NY), employing Cronex Lightning Plus (PerkinElmer) or Biomax MS (Eastman Kodak) intensifying screens. Relative hybridization levels were determined by densitometry and copy number determined by comparing the intensity of the transgenic band to the wild-type band previously defined as one copy. Founder transgenic mice were bred to wild-type CD-1 mice to generate individual transgenic lines. First-generation heterozygous and wild-type littermates were genotyped by Southern blot analysis. Heterozygous mice of subsequent generations were identified by amplification of a 700-bp band by PCR of genomic DNA using 20 μM of a forward primer (5′-ATGGTGCGCACAGCCTACACGGTG-3′), corresponding to bp +1 to bp +24 of gremlin coding sequence, and 20 μM of a reverse primer (5′-TAGAAGGCACAGTCGAGG-3′), corresponding to an 18-bp segment of bovine GH polyadenylation sequence. Heterozygous mice were intercrossed to generate a homozygous offspring, which was identified by Southern blot analysis. The results described were obtained from the analysis of two transgenic lines, derived from independent founders. All animal experiments were approved by the Animal Care and Use Committee of Saint Francis Hospital and Medical Center.

Northern blot analysis

Total RNA was isolated from calvariae using the Trizol reagent solution as per manufacturer's instructions (Invitrogen, Carlsbad, CA). The RNA was resolved by electrophoresis on a formaldehyde agarose gel after denaturation, blotted onto GeneScreen Plus-charged nylon, and hybridized with a 0.6-kb human gremlin cDNA and a 0.7-kb murine 18S ribosomal RNA cDNA from the American Type Culture Collection (Manassas, VA), as described (18). Northern analysis is representative of three samples.

Serology

Serum was collected by intracardiac puncture at the time of killing, and albumin levels were measured using the VITROS ALB Slides quantitative system per manufacturer's instructions (Ortho-Clinical Diagnostics, Rochester, NY).

X-ray analysis and bone mineral density (BMD)

Radiography was performed on mice anesthetized with tribromoethanol (Sigma Chemical Co., St. Louis, MO) on a Faxitron x-ray system (model MX 20, Faxitron X-Ray Corp., Wheeling, IL). The x-rays were performed at an intensity of 35 kW for 25 sec. Total, vertebral, and femoral bone mineral content (BMC; grams), skeletal area (square centimeters), and BMD (grams per centimeter) were measured on anesthetized mice using the PIXImus small animal DEXA system (GE Medical Systems/LUNAR, Madison, WI) (22). Calibrations were performed with a phantom of a defined value, and quality assurance measurements were performed before each use. The coefficient of variation for total BMD is less than 1% (n = 9 mice).

Bone histomorphometric analysis

Static and dynamic histomorphometry was carried out on transgenic mice and wild-type controls at 4.5, 8, and 12 wk of age. Mice were injected with calcein, 20 mg/kg, and 30 mg/kg demeclocycline at an interval of 3, 6, or 8 d for 4.5, 8, and 12-wk-old mice, respectively, and killed by CO_2 asphyxiation 2 d after the demeclocycline injection. Femurs were dissected, fixed in 70% ethanol, dehydrated, and embedded undecalcified in methyl methacrylate. Longitudinal sections, 5 μm thick, were cut on a microtome (Microm, Richards-Allan Scientific, Kalamazoo, MI) and stained with toluidine blue (pH 6.4). Static parameters of bone formation and resorption were measured in a defined area between 181 and 725 μm from the growth plate, using an OsteoMeasure morphometry system (Osteometrics, Atlanta, GA). Cortical width was measured in a segment defined between 725 and 1270 μm from the growth plate. For dynamic histomorphometry, mineralizing surface per bone surface and mineral apposition rate were measured in unstained sections under UV light, using a B-2A set long-pass filter consisting of an excitation filter ranging from 450 to 490 nm, a barrier filter at 515 nm, and a dichroic mirror at 500 nm. Bone formation rate (BFR) was calculated. Polarized-light microscopy was used to analyze the orientation of bone collagen fibrils using a polarizer (Nikon, Inc., Melville, NY). The terminology and units used are those recommended by the Histomorphometry Nomenclature Committee of the American Society for Bone and Mineral Research (23). For determination of mineral content, sections were stained with Von Kossa solution as described previously (24).

Measurement of bromodeoxyuridine incorporation in decalcified bone sections

Transgenic mice and wild-type controls were injected ip with 50 μg bromodeoxyuridine (BrdU) per gram of body weight at 4.5 wk of age, 24 h before being killed. After killing, femurs were dissected, fixed in 10% formalin in PBS for 3 h at room temperature, decalcified with Decal-Stat (Decal Corp., Tallman, NY) overnight at 4 C, and embedded in paraffin. Longitudinal sections across the femurs were obtained. Before processing, tissue slides were exposed to 0.05% pepsin in 0.1 N HCl for 30 min at 37 C. Slides were then placed in citrate buffer, heated at 50 C for 20 min for heat-induced target antigen retrieval, and incubated with 1:100 primary antibody to BrdU (Dako Corp., Carpinteria, CA) (25, 26). To identify actively proliferating cells, nuclei that had incorporated BrdU were detected using the EnVision+ System, peroxidase (diaminobenzidine) system (Dako) per manufacturer's instructions. Sections were counterstained with hematoxylin. For each section, BrdU-positive nuclei of cells lining the trabecular perimeter were counted in three consecutive fields of the primary spongiosa. Two sections were counted for each of three wild-type and four transgenic mice. Sections incubated in the absence of the primary antibody were used as

negative controls for the assay. Preliminary experiments confirmed absence of BrdU-positive cells in mice injected with vehicle alone.

Measurement of apoptosis in undecalcified bone sections

Sections were mounted on poly-lysine-coated glass slides (Allegiance Healthcare Corp., McGraw Park, IL). Slides were treated with 100 μl of 20 μg/μl proteinase K in 10 mM Tris (pH 8.0) for 20 min at room temperature, rinsed twice with 50 mM Tris-buffered saline (TBS) [0.05 M Tris, 0.138 M NaCl, 0.0027 M KCl (pH 8.0)] for 5 min and once in 10 mM TBS (pH 7.6), reincubated in 30% H_20_2 in methanol for 4 min, and rinsed with 50 mM TBS. DNA fragmentation was detected by the transferase-mediated digoxigenin-deoxyuridine triphosphate *in situ* nick-end labeling reaction using Klenow terminal deoxynucleotidyl transferase per manufacturer's instructions (Oncogene Research Products, Cambridge, MA) (27). Sections were incubated in 0.15% $CuSO_4$ in 0.9% NaCl for 2 min and counterstained with 2% methyl green aqueous solution. Sections of femurs and calvariae from wild-type mice treated with 1 μg/μl DNase I in 50 mM TBS and 1 mM $MgSO_4$ were used as a positive control of the assay. Sections not incubated with the transferase, but with vehicle alone, were used as negative controls. Cells in which the nuclei were clearly dark brown rather than blue green were considered apoptotic, and osteoblasts were identified as cells lining the trabecular surface.

Bone marrow stromal cell cultures

Femurs were aseptically removed from 4.5-wk-old mice, after CO_2 asphyxiation, and stromal cells were recovered by centrifugation, as described (28). Cells were plated at a density of 5×10^5 cells/cm^2 and cultured in αMEM (Invitrogen, Rockville, MD) containing 15% fetal bovine serum (FBS) (Atlanta Biologicals, Norcross, GA) at 37 C in a humidified 5% CO_2 incubator. Half the volume of the culture medium was replaced after 4 d of culture with fresh medium, and when wild-type cells reached confluence (6–7 d of culture), the medium was changed to αMEM supplemented with 10% FBS, 50 μg/ml ascorbic acid, and 5 mM β-glycerophosphate (Sigma) in the absence or presence of recombinant human BMP-2 (Wyeth, Collegeville, PA). The medium was replaced twice a week for the duration of the culture, and cells were harvested 3 d after the last change of medium. For cytochemical analysis, cells were fixed with 4.5 mM citric acid, 2.25 mM sodium citrate, 65% acetone, and 8% formalin and stained for the presence of mineralized nodules using 2% alizarin red (Sigma) (28). To assess changes in cell number, cultures were trypsinized, cells suspended in PBS, and viable cells counted under the microscope after trypan blue staining. Data are expressed as number of cells per well and are obtained from two distinct cultures. To assess changes in phosphorylated mothers against decapentaplegic (Smad) phosphorylation and β-catenin levels, cells were cultured for 10 d; serum deprived overnight; and exposed to control medium, BMP-2, or human recombinant TGFβ1 (Genentech, South San Francisco, CA) for 20 min, as indicated in text and legends.

To evaluate changes in osteoclastogenesis, stromal cells were plated at 2.5×10^5 cells/cm^2 and cultured in αMEM medium containing 10% FBS in the presence of 10 nM 1,25 dihydroxy vitamin D_3. To determine the number of tartrate-resistant acid phosphatase-positive multinucleated cells, cultures were fixed and stained using an acid phosphatase staining kit according to manufacturer's instructions (Sigma) (29).

RT-PCR

Total RNA was isolated from stromal cells and 2 μg were DNase I treated and reverse transcribed with murine Moloney leukemia virus reverse transcriptase (Invitrogen) in the presence of 20 μM random primers. To quantify gremlin transgene, 0.1 μg reverse-transcribed DNA was amplified by 26 PCR cycles at 54 C annealing temperature in the presence of 20 μM of a forward primer corresponding to bp +1 to bp +24 of gremlin coding sequence and 20 μM of a reverse primer corresponding to an 18-bp segment of bovine GH polyadenylation sequence present in the osteocalcin-gremlin construct, both described in *Generation of transgenic mice*. To measure osteocalcin transcripts, 0.1 μg reverse-transcribed DNA was amplified by 28 PCR cycles at 55 C annealing temperature in the presence of 20 μM of a forward primer (5′-ACCAGTATGGCTTGAAGACCGC-3′) and 20 μM of a reverse primer (5′-TTTTGGAGCTGCTGTGACATCC-3′). To control for the amount of DNA amplified, 18S was coamplified in the same reaction using 20 μM of a forward primer (5′-ATGTCTAAGTACGCACGG-3′) and 20 μM of a reverse primer (5′-AGCGACCAAAGGAACCATA-3′).

Western immunoblot analysis

To determine phosphorylated Smads, the cell layer was extracted from stromal cells in a lysis buffer of 20 mM Tris (pH 7.4), 150 mM NaCl, 1% P40, and 1 mM EDTA in the presence of protease inhibitors. Seventy micrograms of total cellular protein were fractionated by polyacrylamide gel electrophoresis in 12% gels under nonreducing conditions and transferred to Immobilon P membranes (Millipore, Bedford, MA). For phosphorylated Smad 1/5/8, the membranes were blocked with 2% BSA in PBS and exposed to a 1:1000 dilution of a polyclonal antibody that recognizes Smad 1, 5, and 8 phosphorylated at the last two serine residues (Dr. C. H. Heldin, Ludwig Institute for Cancer Research, Uppsala, Sweden, and Dr. P. ten Dijke, The Netherlands Cancer Institute, Amsterdam, The Netherlands) or a 1:1000 dilution of an antibody to unphosphorylated Smad 5 (Cell Signaling Technologies, Beverly, MA) (30). For Smad 2, the membranes were blocked with 5% nonfat dry milk in TBS and 0.1% Tween (pH 7.6) and exposed to a 1:1000 dilution of a polyclonal antibody to phosphorylated Smad 2 (Ser465/467) or unphosphorylated Smad 2 (Cell Signaling Technology). To determine β-catenin levels, the cell layer was extracted in 10 mM Tris, 140 mM NaCl, 5 mM EDTA, and 2 mM dithiothreitol buffer at pH 7.6 in the presence of protease inhibitors and the cytosolic fraction separated by ultracentrifugation as described (31). Seventy micrograms of total cytosolic protein were fractionated by PAGE in 7.5% gels under nonreducing conditions and transferred to Immobilon P membranes. Membranes were blocked with 2% BSA in PBS and exposed to a 1:1000 dilution of a monoclonal antibody to unphosphorylated β-catenin (Santa Cruz Biotechnology, Santa Cruz, CA) or a 1:1000 dilution of a polyclonal antibody to β-actin (Cell Signaling Technology). Blots were exposed to antirabbit or antimouse IgG antiserum conjugated to horseradish peroxidase and developed with a chemiluminescence detection reagent (PerkinElmer).

ST-2 cell cultures and transient transfections

ST-2 cells, cloned stromal cells isolated from bone marrow of BC8 mice (Dr. S. Harris, University of Texas Health Sciences Center, San Antonio, TX) were grown in a humidified 5% CO_2 incubator at 37 C in αMEM, supplemented with 10% FBS (32). To determine changes in BMP-2 signaling, a construct containing 12 copies of a Smad 1/5 response element, linked to the osteocalcin basal promoter, and cloned upstream of a luciferase reporter gene (12× SBE-OC-pGL3) (Dr. M. Zhao, University of Texas Health Sciences Center, San Antonio, TX) was tested in transient transfection experiments (33). To determine changes in β-catenin transactivating activity, a pTOPFLASH reporter construct containing three copies of the lymphoid enhancer binding factor 1/T-cell transcription factor 4 binding sequences, CCTTTGATC, or its mutant, pFOPFLASH, containing three copies of the mutant binding site, CCTTGGCC, both cloned upstream of a minimal c-*fos* promoter and a luciferase reporter gene (Dr. J. Kitajewski, New York University, New York City, NY) were tested in transient cotransfections in the presence of a Wnt 3/pUSE expression construct (Dr. J. Billiard, Wyeth) or a pcDNA3.1 vector (34). ST-2 cells were cultured to 70% confluence and transiently transfected with the indicated constructs using FuGene6 (3 μl FuGene/2 μg DNA) according to manufacturer's instructions (Roche, Indianapolis, IN). Cotransfections with a β-galactosidase expression construct (Clontech, San Jose, CA) were used to control for transfection efficiency. Cells were exposed to the FuGene-DNA mix for 16 h; transferred to serum-containing medium for 8 h; serum deprived overnight and treated for 24 h with control medium, BMP-2, recombinant murine gremlin (R&D Pharmaceuticals, Minneapolis, MN), or recombinant human noggin (Regeneron Pharmaceuticals); and harvested. Luciferase and β-galactosidase activities were measured using an Optocomp luminometer (MGM Instruments, Hamden, CT). Luciferase activity was corrected for β-galactosidase activity to control for transfection efficiency.

Statistical analysis

Results are expressed as means ± SEM. Statistical significance was determined by ANOVA.

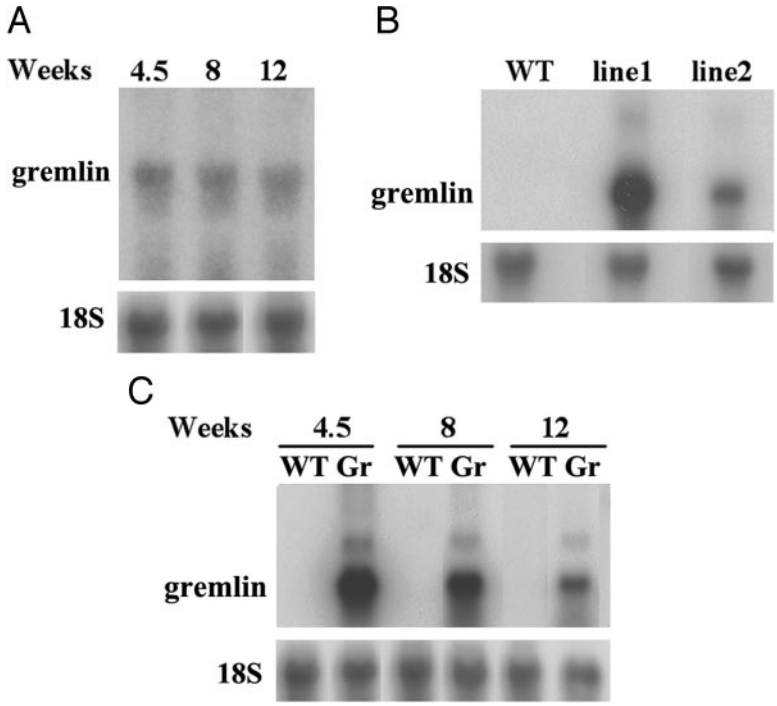

FIG. 1. Gremlin mRNA expression in calvariae of wild-type (WT) mice and relative levels of expression of gremlin transgene mRNA in gremlin transgenic mice (Gr) and wild-type controls. To determine the expression of gremlin in wild-type calvariae, total RNA was extracted from calvariae of 4.5-, 8-, and 12-wk-old wild-type mice (A). To determine the expression of the gremlin transgene, total RNA was extracted from calvariae of 4.5-wk-old heterozygous gremlin transgenic mice from line 1 and homozygous gremlin transgenic mice from line 2 (B) or from line 1 transgenic mice and wild-type controls at 4.5, 8, and 12 wk of age (C). RNA was resolved by Northern blot analysis and hybridized with [α-^{32}P]-labeled human gremlin and mouse 18S cDNAs.

Results

Generation, identification, and overall phenotype of gremlin transgenic mice

Two transgenic mouse lines overexpressing gremlin under the control of the rat osteocalcin promoter were generated. Founder 1 carried 20 copies of the transgene, and attempts to generate a homozygous offspring were unsuccessful, suggesting that high levels of gremlin expression may compromise viability. However, there was no evidence of heterozygous lethality after heterozygote-wild-type matings, which generated the expected mendelian ratio of 50% heterozygous to 50% wild-type offspring. Founder 2 carried four to six copies of the transgene and was used to generate a homozygous offspring expressing eight to 12 copies of the transgene. Endogenous gremlin transcripts (4.5 kb) were expressed in RNA extracted from calvariae of wild-type controls at 4.5, 8, and 12 wk of age (Fig. 1A). Gremlin transgene (0.9 kb) was expressed in both transgenic lines (Fig. 1B); high levels of the transgene were detected at 4.5 wk and then declined as the animals aged (Fig. 1C), corresponding to the decrease in activity of the rat osteocalcin promoter in older mice (35, 36). Both transgenic lines displayed analogous skeletal phenotypes and transgenic mice from founder 1 were studied in more detail and were used for *in vitro* experiments. Transgenic mice were compared with wild-type age-matched controls at 4.5, 8, and 12 wk of age.

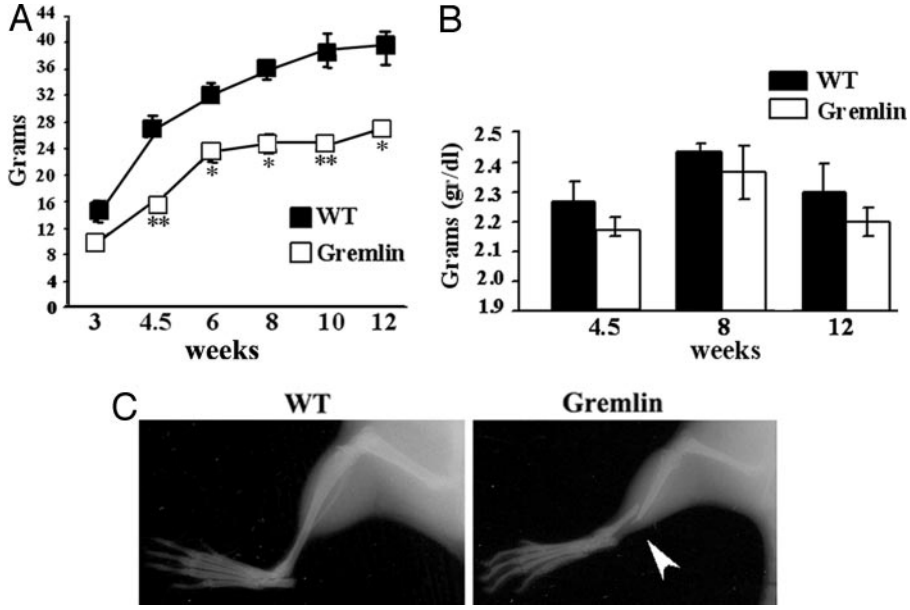

FIG. 2. Gremlin overexpression leads to a decrease of body weight through a 12-wk period of study and causes spontaneous fractures. The weight of gremlin transgenic mice (*white squares*) and wild-type (WT) controls (*black squares*) was analyzed from 3 to 12 wk. Values are means ± SEM; n = 6–12 (A). *, Significantly different from wild-type controls, $P < 0.05$; **, significantly different from wild-type controls, $P < 0.001$. Serum albumin levels were measured in gremlin transgenic mice (*white bars*) and wild-type controls (*black bars*) at 4.5–12 wk of age. Values are means ± SEM; n = 3 (B). A representative skeletal radiograph demonstrates a fracture in a 4.5-wk-old gremlin transgenic mouse (*arrowhead*) (C).

TABLE 1. Total BMC (g), skeletal area (cm^2), and BMD (g/cm^2) were obtained from 4.5-, 8-, and 12-wk-old gremlin transgenic mice and wild-type controls

Weeks	BMC		Skeletal area		BMD	
	Wild type	Gremlin	Wild type	Gremlin	Wild type	Gremlin
4.5	0.350 ± 0.01	0.244 ± 0.02[a]	7.7 ± 0.5	6.8 ± 0.2[a]	0.045 ± 0.002	0.036 ± 0.002[a]
8	0.476 ± 0.03	0.386 ± 0.02[a]	9.1 ± 0.5	8.4 ± 0.3[a]	0.054 ± 0.001	0.042 ± 0.002[a]
12	0.565 ± 0.02	0.370 ± 0.03[a]	9.2 ± 0.6	7.9 ± 0.6[a]	0.060 ± 0.001	0.047 ± 0.002[a]

Values are means ± SEM; n = 6–11.
[a] Significantly different from wild-type controls, $P < 0.001$.

At birth, gremlin-overexpressing mice were indistinguishable from wild-type controls, but at 1.5–2 wk of age, they appeared smaller. At 4.5 wk of age, the weight of transgenics was reduced by approximately 35%, a decrease sustained through the 12 wk of observation (Fig. 2A). In accordance with the activity of the osteocalcin promoter in odontoblasts, gremlin overexpression caused tooth fragility (37). Inferior incisors erupted normally, but fractured, so that upper incisors grew unopposed, interfering with mouth occlusion. To avoid feeding difficulties leading to malnutrition, upper incisors were trimmed weekly, and granular, easily chewable food was administered. Serum albumin levels of gremlin overexpressing mice were not significantly reduced, excluding the presence of severe protein-caloric malnutrition (Fig. 2B) (38). The phenotype of gremlin transgenic mice appeared limited to the skeleton, and in both transgenic lines, the observed skeletal changes were similar in males and females.

X-rays and BMD

Contact radiography of gremlin transgenics confirmed the reduction in body size and revealed severe osteopenia and the presence of spontaneous fractures, which at 4.5 wk of age were detected in tibiae and humeri but not in other bones. Fractures of the tibiae were the most frequent, were often bilateral, and were noted in virtually all gremlin-overexpressing mice (Fig. 2C). In accordance with the x-ray findings, gremlin-overexpressing mice had significant and sustained decreases in BMC and BMD when compared with wild-type controls. At 4.5–12 wk of age, total BMC was 19–35% and total BMD was 20% lower in transgenics than in wild-type controls (Table 1). The decrease in BMC and BMD was generalized and observed in femoral and vertebral bones. At 4.5 wk of age, the decrease in transgenic mice was 21 and 32% for femoral and vertebral BMD, respectively, an effect that was sustained throughout the 12-wk period of study (Table 2).

Static and dynamic histomorphometry

Gremlin overexpression caused a profound distortion of cortical and trabecular bone structure and an inhibition of bone remodeling. The femoral length and middiaphysis width of transgenic mice were reduced by about 20 and 50%, respectively, throughout the 12-wk period of study. Femurs from gremlin transgenics exhibited an early increase in cortical width and decrease in trabecular bone volume and number. The cortical bone was characterized by disorganized trabeculae, which appeared to extend into the marrow space in the metaphysial region. The increased cortical thickness and reduced bone width resulted in a narrowing of the medullary cavity often leading to fusion and distortion of skeletal architecture. At 4.5 wk of age, histomorphometric analysis of femurs from gremlin transgenic mice revealed a 40% decrease in trabecular bone volume, secondary to a decreased number and thickness of trabeculae (Figs. 3A and 4). At 8 and 12 wk, trabecular bone volume was not different between gremlin transgenic and wild-type control mice, possibly because of a decline in the activity of the osteocalcin promoter. Gremlin transgenics exhibited a 70% reduction in the number of osteoblasts per trabecular area, indicating a role of gremlin either in the regulation of cell proliferation or survival of cells of the osteoblastic lineage (Fig. 4). Although the effect on osteoblast number was sustained, it was less pronounced at 8 and 12 wk of age. In parallel to the decrease in the number of osteoblasts, an initial decrease of approximately 50% in the number of osteoclasts was observed indicating, in association with dynamic histomorphometric data, a state of decreased bone remodeling (39, 40).

Fluorescence microscopy of gremlin transgenic mice revealed diffuse broad bands of the fluorescent labels, features characteristic of woven bone (Fig. 3B). Mineralization fronts were visible in only a few isolated trabecular and cortical areas, which were used to estimate the mineralizing surface, mineral apposition, and BFRs. These were reduced significantly in gremlin transgenics at 4.5–12 weeks of age (Fig. 4). Polarized-light microscopy confirmed the presence of woven bone with an abundance of disorganized and thin collagen bundles and a marked reduction of mature lamellar bone (Fig. 3C). Von Kossa staining failed to reveal appreciable differences in mineral content between gremlin and control mice. At 4.5 weeks of age, gremlin transgenics exhibited a

TABLE 2. BMD was obtained from 4.5-, 8-, and 12-wk-old gremlin transgenic mice and wild-type controls

Weeks	Total BMD		Vertebral BMD		Femoral BMD	
	Wild type	Gremlin	Wild type	Gremlin	Wild type	Gremlin
4.5	0.045 ± 0.002	0.036 ± 0.002[a]	0.068 ± 0.004	0.046 ± 0.004[a]	0.049 ± 0.001	0.039 ± 0.003[a]
8	0.054 ± 0.001	0.042 ± 0.002[a]	0.083 ± 0.005	0.064 ± 0.006[a]	0.060 ± 0.002	0.048 ± 0.002[a]
12	0.060 ± 0.001	0.047 ± 0.002[a]	0.060 ± 0.002	0.048 ± 0.002[a]	0.089 ± 0.007	0.066 ± 0.006[a]

BMD is expressed as g/cm^2 and values are means ± SEM; n = 6–11 of total, vertebral and femoral BMD.
[a] Significantly different from wild-type controls, $P < 0.001$.

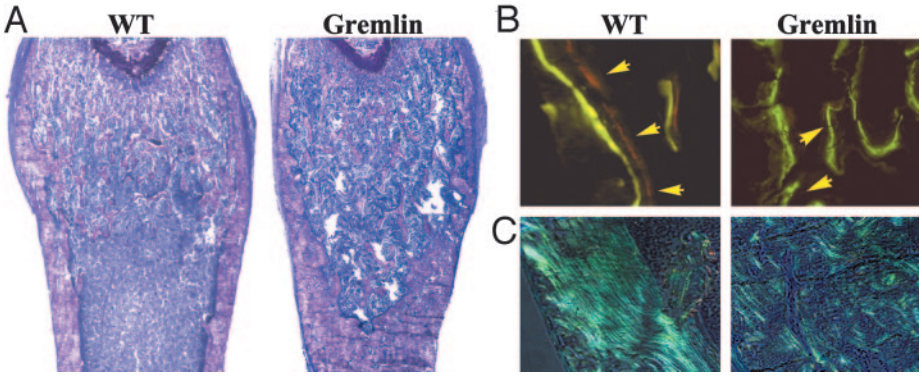

FIG. 3. Gremlin overexpression affects cortical and trabecular bone, inhibits bone formation, and causes woven bone. Histological sections from 4.5-wk-old gremlin transgenic mice and wild-type (WT) controls were stained with toluidine blue (A). Final magnification, ×40. Sections from 4.5-wk-old gremlin transgenics and wild-type controls, given sequential injections of calcein and demeclocycline (*arrows*) were visualized by fluorescence microscopy (B) or by polarized light microscopy (C). Final magnification, ×100.

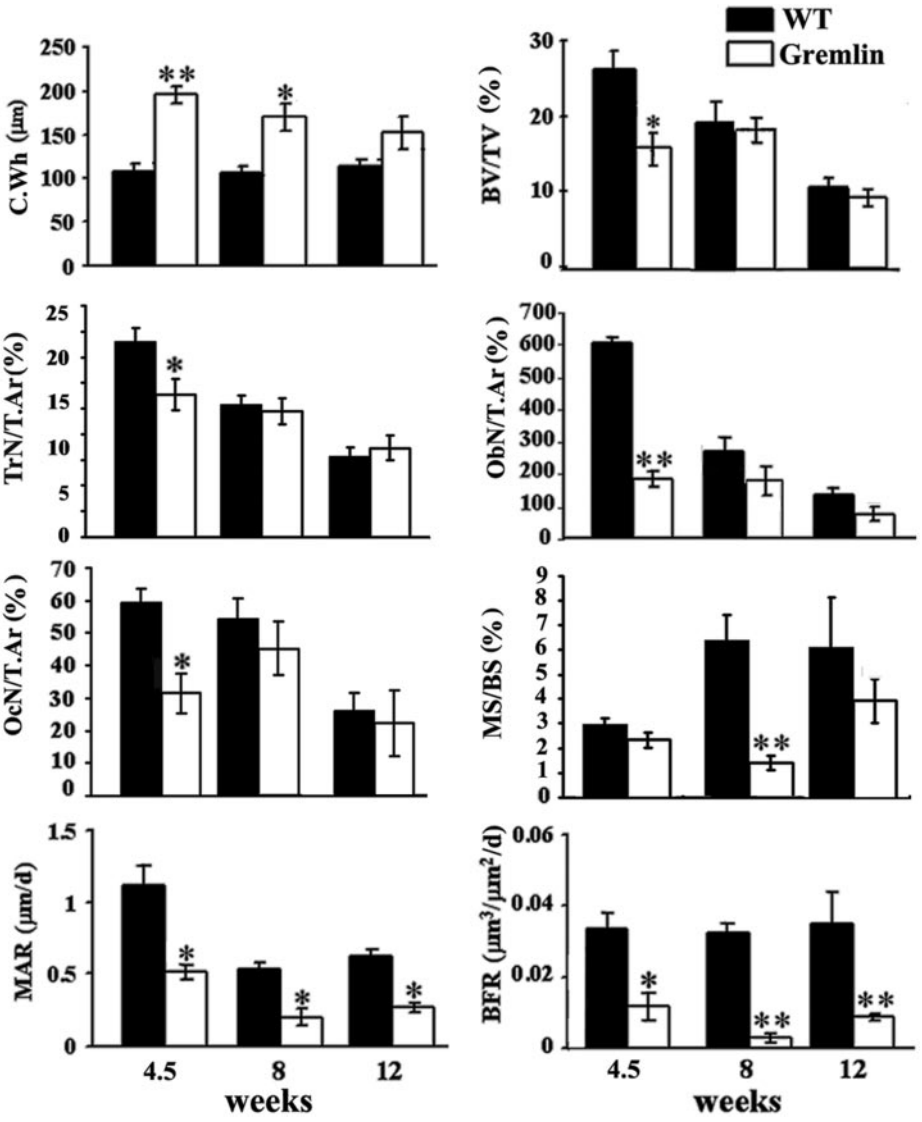

FIG. 4. Gremlin overexpression increases cortical width (C.Wh), decreases trabecular bone volume (BV/TV) and trabecular number (TrN.Ar), and reduces the number of osteoblasts (ObN/T.Ar) and osteoclasts (OcN/T.Ar) per trabecular area, mineralizing surface per bone surface (MS/BS), mineral apposition rate (MAR), and BFR. Bone histomorphometry was performed on femurs from 4.5-, 8-, and 12-wk-old gremlin transgenic mice (*white bars*) and wild-type (WT) controls (*black bars*). For static histomorphometry, sections were stained with toluidine blue. For dynamic histomorphometry, unstained sections were analyzed by fluorescence microscopy. Values are means ± SEM; n = 6–11. *, Significantly different from wild-type controls, $P < 0.05$; **, significantly different from wild-type controls, $P < 0.001$.

TABLE 3. Femoral bone histomorphometry in 4.5-wk-old gremlin transgenic mice and wild-type controls from line no. 2

	Wild type	Gremlin
Trabecular relative bone volume (%)	15.4 ± 0.7	11.3 ± 0.6[a]
Osteoblast surface/bone surface (%)	17.8 ± 1.0	15.7 ± 0.9
Number of osteoblasts/ trabecular area (mm^2)	530.4 ± 31.8	338.5 ± 30.3[a]
Osteoclast surface/bone surface (%)	7.4 ± 0.4	6.0 ± 0.4[a]
Number of osteoclasts/ trabecular area (mm^2)	113.9 ± 8.6	76.2 ± 7.3[a]
Trabecular thickness (μm)	15.1 ± 0.4	14.3 ± 0.6
Trabecular number (per mm)	10.3 ± 0.7	8.1 ± 0.8
Trabecular separation (μm)	84.7 ± 6.4	113.9 ± 9.2[a]
Cortical thickness (μm)	106.2 ± 3.5	180.4 ± 10.6[a]
Mineralizing surface/bone surface (%)	1.8 ± 0.3	1.0 ± 0.5
Mineral apposition rate (μm/d)	0.40 ± 0.05	0.24 ± 0.03[a]
Bone formation rate ($\mu m^3/\mu m^2$·d)	0.0072 ± 0.001	0.0038 ± 0.002[a]

Values are means ± SEM; n = 6.
[a] Significantly different from wild-type controls, $P < 0.05$.

nonstatistically significant 16% decrease in the height of the growth plate, and its architecture appeared normal.

To investigate whether the reduction in the number of osteoblasts in gremlin transgenics was secondary to a decrease in cell proliferation, 4.5-wk-old gremlin transgenic mice and wild-type controls were killed 24 h after an ip injection of BrdU. The number of BrdU-labeled osteoblasts per trabecular area was 14.6 ± 4.4 cells/mm^2 (means ± SEM; n = 3) in transgenics and 32.7 ± 1.3 cells/mm^2 in wild-type controls ($P < 0.001$). There was no detectable difference in the number of apoptotic osteoblasts, as determined by the transferase-mediated digoxigenin-deoxyuridine triphosphate *in situ* nick-end labeling assay in femurs from 4.5-wk-old gremlin transgenic mice and wild-type controls (not shown).

Homozygous gremlin transgenic mice from line 2 and wild-type controls were analyzed by static and dynamic histomorphometry at 4.5 wk of age. Similar to line 1, gremlin transgenics displayed a decrease in trabecular bone volume, number of osteoblasts and osteoclasts per trabecular area, and BFR (Table 3). The increase in cortical thickness and reduction in mature lamellar bone observed in line 1 were also observed. In accordance with the lower levels of the transgene transcripts in line 2, their skeletal phenotype was less pronounced than in line 1.

Primary stromal cell cultures

To investigate the effect of gremlin on osteoblastic cell replication and function, stromal cells from 4.5-wk-old transgenic mice and wild-type controls were cultured in differentiation medium in the absence or presence of BMP-2 at 1 nM for 21 d. Stromal cells from gremlin transgenic, but not from wild-type mice, expressed the gremlin transgene, as determined by RT-PCR. The transgene was expressed 10 d after plating, and its levels were maintained through the 21 d of culture (Fig. 5A). Stromal cells from gremlin transgenics and wild-type control mice were plated at the same density, but when stromal cells from wild-type mice reached confluence (7 d), cultures from gremlin transgenics contained about

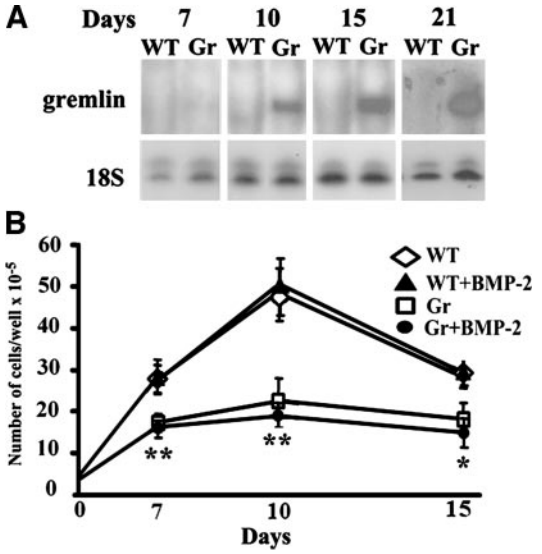

FIG. 5. Gremlin overexpression reduces the number of viable cells. Bone marrow stromal cells from 4.5-wk-old gremlin transgenic mice (Gr) and wild-type (WT) controls were isolated and plated at equal density (d 0), and 7 d later they were switched to differentiation medium. A, Cells were cultured in the absence of BMP, and total RNA was extracted at the indicated days, 2 μg were reverse transcribed, and 0.1 μg was amplified by PCR with specific primers for gremlin transgene (700 bp) and 18S (79 bp) in the presence of [α-^{32}P]dCTP. RT-PCR is representative of three cultures. B, Cells from wild-type and transgenics were cultured continuously in the absence (◇, wild-type, □, gremlin) or presence (▲, wild type; ●, gremlin) of BMP-2 at 1 nM started 7 d after plating. Cell number was determined in trypsinized cellular extracts and is expressed as total viable cells per well. Values are means ± SEM; n = 5. The experiment was performed twice with analogous results. *, Significantly different from wild-type controls, $P < 0.05$; **, significantly different from wild-type controls, $P < 0.001$.

two thirds the number of cells. The decrease cellularity was observed before the detection of the gremlin transgene *in vitro*, suggesting that it was secondary to previous *in vivo* exposure of the cells to gremlin. As the cultures progressed, those from gremlin transgenics exhibited a 50% decrease in the number of viable cells (Fig. 5B). Confirming prior observations, BMP-2 did not cause an increase in cell number in wild-type cells, and it did not rescue gremlin negative impact on cell proliferation (41). Osteocalcin transcripts were detected in wild-type cells at 10 d, and they were maintained as the cells formed mineralized nodules. Stromal cells overexpressing gremlin displayed a delay in the expression of osteocalcin mRNA and did not mineralize (Fig. 6). The effect of gremlin on mineralized nodule formation was reversed by BMP-2, which stimulated the formation of mineralized nodules at 21 d of culture. BMP-2 caused a modest increase in osteocalcin transcripts but did not reverse the suppression caused by gremlin overexpression (Fig. 6, A and B).

To examine the impact of gremlin on osteoclastogenesis, bone marrow stromal cells from gremlin transgenics and wild-type control mice were cultured for 6 d in the presence of 10 nM 1,25 dihydroxy vitamin D_3. Gremlin overexpression led to a 50% reduction in the number of tartrate-resistant acid phosphatase-positive multinuclear cells from 26.8 ± 4.4 cells/well (means ± SEM; n = 6) in wild-type cultures to 10.8 ± 2.4 cells/well in transgenics ($P < 0.01$).

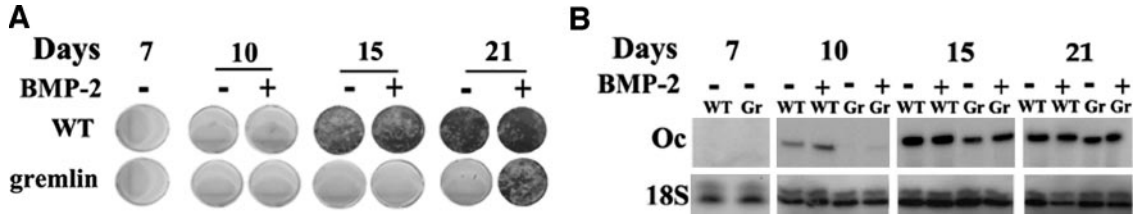

FIG. 6. Gremlin overexpression inhibits osteoblastogenesis. Bone marrow stromal cells from 4.5-wk-old gremlin (Gr) transgenic mice and wild-type (WT) controls were plated (d 0), and 7 d later they were switched to differentiation medium in the absence (−) or presence (+) of BMP-2 at 1 nM. A, Cells were stained at the indicated times with alizarin red to estimate mineralized nodule formation. B, Total RNA was extracted, 2 μg were reverse transcribed, and 0.1 μg was amplified by PCR with specific primers for osteocalcin (Oc, 219 bp) and 18S (79 bp) in the presence of [α-^{32}P]dCTP. RT-PCR is representative of three cultures.

To explore mechanisms involved in the determination of the phenotype described, stromal cells from transgenic mice were cultured for 10 d and tested for Smad phosphorylation after treatment with BMP-2 at 1 nM for 20 min. Transgenic cells displayed a decreased response to BMP-2 on Smad 1/5/8 phosphorylation, confirming that gremlin-overexepressing cells inhibit BMP signaling (Fig. 7A). Gremlin effects were specific to BMP, and stromal cells from transgenic mice displayed normal Smad 2 phosphorylation after treatment with TGFβ at 200 pM for 20 min (Fig. 7B) (1). The impact of gremlin on Wnt signaling also was investigated because Cerberus, a member of the DAN family with an 85% amino acid homology with gremlin, binds and inhibits Wnt signaling (42). Stromal cells from gremlin transgenics, cultured for 10 d, exhibited a 50% reduction in free cytosolic β-catenin levels when compared with wild-type controls, indicating that the Wnt canonical signaling was impaired (Fig. 7C).

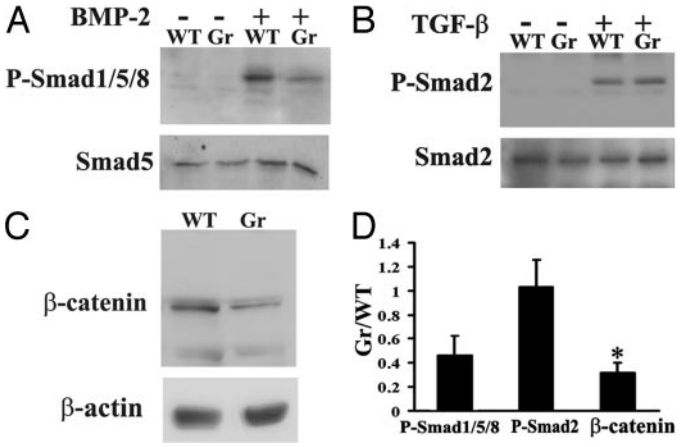

FIG. 7. Gremlin overexpression causes a reduced response to BMP on Smad 1/5/8 phosphorylation, but not to TGFβ on Smad 2 phosphorylation and causes decreased levels of free cytosolic β-catenin. Bone marrow stromal cells from 4.5-wk-old gremlin transgenic mice (Gr) and wild-type control (WT) were cultured, and 7 d after plating, they were switched to differentiation medium. Ten days after plating, cells were serum deprived overnight. For Smad phosphorylation, cells were tested with BMP-2 at 1 nM or TGFβ at 200 pM for 20 min. Total cellular extracts were processed for Western immunoblot analysis and exposed to an antibody to phospho-Smad 1/5/8 or phospho-Smad 2. Membranes were also incubated with antibodies to unphosphorylated Smad 5 and 2 to control for protein loading (A and B). For determination of cytosolic β-catenin levels, total cytosolic extracts were resolved by Western immunoblot analysis and exposed to an antibody to free β-catenin or an antibody to β-actin to control for protein loading (C). The graph represents fold changes of gremlin stromal cultures/wild-type. Values are means ± SEM; n = 3 (D). *, Significantly different from wild-type, $P < 0.05$.

ST-2 cell cultures

To compare the effects of gremlin and noggin on BMP-2/Smad and Wnt/β-catenin signaling, ST-2 cells, a line of murine stromal cells, which differentiate into functional osteoblasts in the presence of BMP-2, was employed (28). ST-2 cells were transiently transfected with the β-catenin-responsive construct pTOPFLASH or its mutant pFOPFLASH and a Wnt 3 expression vector or a pcDNA3.1 vector control. Eighteen hours after the transfection, cells were treated with gremlin or noggin at 1–30 nM for 24 h. Wnt 3 cotransfection increased pTOPFLASH activity by 20-fold, and this effect was inhibited by noggin and gremlin at the doses tested (Fig. 8A). These data confirm gremlin down-regulation of Wnt activation of the β-catenin canonical pathway and suggest that this effect is not direct and specific to the gremlin peptide but possibly associated to the BMP antagonistic activity of noggin and gremlin. As expected, BMP-2 stimulated the activity of the 12× SBE-OC-pGL3 luciferase reporter construct transiently transfected into ST-2 cells by 10-fold, and this effect was blocked equally by gremlin and noggin at the doses tested (Fig. 8B).

Discussion

Our findings demonstrate that transgenic mice overexpressing the BMP antagonist gremlin, under the control of the osteocalcin promoter, develop a decrease in body size, tooth fragility, spontaneous fractures, modeling defects of long bones, and severe osteopenia. The skeletal phenotype was evident at 4.5 wk of age, a time of marked expression of the transgene, although bone formation rate and BMD were reduced over the 12-wk period of study. Gremlin overexpression altered the trabecular and cortical bone structure, leading to a severe distortion of skeletal architecture. Histomorphometric analysis of femurs from gremlin transgenic mice revealed reduced trabecular bone volume in the metaphysis and poorly mineralized woven bone in the middiaphysis. The absence of mature lamellar bone and the presence of disorganized bone could explain the occurrence of spontaneous fractures and the structural distortion.

Osteoblast-targeted gremlin overexpression caused an inhibition of bone formation possibly by different mechanisms. In line with previous work suggesting a role for the rat homologue of gremlin, *drm*, in the regulation of cell growth,

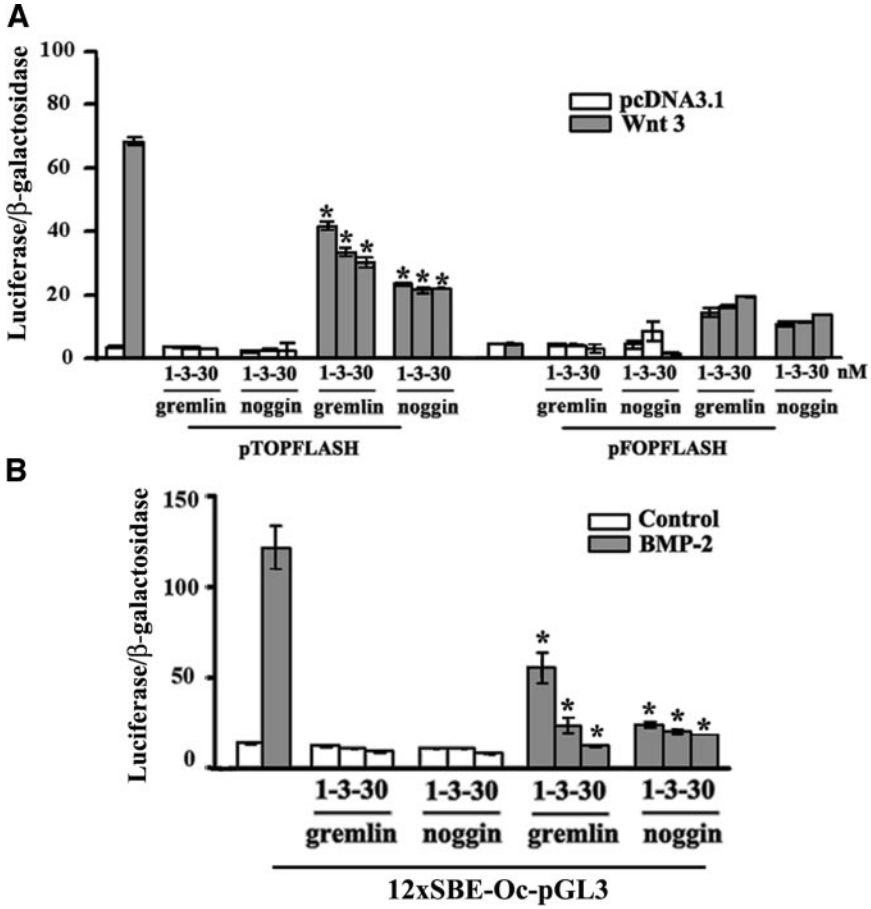

FIG. 8. Gremlin and noggin inhibit Wnt/β-catenin and BMP/Smad signaling. A, Subconfluent cultures of ST-2 cells were transiently cotransfected with pTOPFLASH or its mutant pFOPFLASH and a CMV-β-galactosidase expression construct. Where indicated, pcDNA3.1 (*white bars*) or Wnt 3 (*gray bars*) expression constructs were added to the transfection mix. Sixteen hours after the transfection, cells were serum deprived overnight and treated with gremlin (1–30 nM) or noggin (1–30 nM) for 24 h. B, Subconfluent ST-2 cells were transiently cotransfected with a 12× SBE-Oc-pGL3 or pGL3 (not shown) and a cytomegalovirus-β-galactosidase expression construct. Sixteen hours after the transfection, cells were serum deprived overnight and switched to control medium (*white bars*) or BMP-2 at 1 nM (*gray bars*) in the absence or presence of gremlin (1–30 nM) or noggin (1–30 nM). Data shown represent luciferase/β-galactosidase activity and are means ± SEM; n = 4–6 observations. *, Significantly different from Wnt 3 (A) or BMP-2 (B), $P < 0.001$.

gremlin transgenic mice displayed a reduction in the replication of cells of the osteoblastic lineage. In addition to a possible direct effect on cell proliferation, gremlin could have prevented the differentiation of mesenchymal stem cells toward mature osteoblasts by blocking the effects of BMP on surrounding pluripotent mesenchymal cells. Analysis of osteoblast gene markers in bone marrow stromal cell cultures revealed a decrease in osteocalcin transcripts in gremlin overexpressing cells, indicating an inhibition on osteoblastic cell function. Previous results *in vitro* demonstrated that addition of gremlin to primary osteoblasts prevents the stimulatory effects of BMP on alkaline phosphatase and collagen synthesis (18). Consistent with a decrease in functional osteoblasts, osteoclast number *in vivo* was transiently reduced, and osteoclastogenesis from bone marrow-derived precursor cells *in vitro* was inhibited by 50%. Gremlin overexpression caused, therefore, a generalized decrease in bone remodeling, which could explain the architectural alterations observed in the appendicular skeleton. Femurs from gremlin transgenics were characterized by increased cortical thickness and reduced bone width, which resulted in a narrowing of the medullary cavity often leading to fusion. The rat osteocalcin is active in newborns and seems to be highly efficient at 4 wk of age, followed by a decline in activity. It is our hypothesis that gremlin overexpression in the first weeks of life could have inhibited periosteal new bone formation and endosteal bone resorption, thus blocking the increase in diameter of the marrow cavity and the transition from immature woven to organized lamellar bone in the growing skeleton.

Gremlin is expressed in osteoblasts and binds and blocks the actions of BMP-2, -4, and –7, which play a key role in the regulation of bone function and fracture repair (33, 44–48). BMP-2, -4, and -7 induce the differentiation of pluripotent marrow stromal cells into osteoblasts and enhance the function of differentiated osteoblastic cells. They stimulate the synthesis of extracellular matrix proteins, down-regulate the secretion of matrix metalloproteases, and accelerate the process of bone mineralization (1, 49). Previous work from our laboratory reported that transgenic mice overexpressing the BMP antagonist noggin under the control of the osteocalcin promoter exhibit severe osteopenia, fractures, and a profound decrease in bone formation (19). However, the skeletal phenotypes of gremlin and noggin transgenic mice are not the same. Whereas noggin overexpression causes a severe inhibition of trabecular bone volume, the effect appears to be due primarily to a decrease in osteoblast function and not number. The reasons for the different phenotypes are not immediately apparent because both noggin and gremlin bind and inhibit the actions of BMP-2, -4, and -7, although noggin binds these BMPs with higher affinity than gremlin (1, 46). Gremlin additional effects, and the only partial rescue of the cellular phenotype by the addition of BMP to stromal cells from gremlin transgenics, would suggest direct actions of gremlin in skeletal cells or activities mediated by interactions with other members of the TGFβ superfamily of

peptides. We questioned whether gremlin could alter TGFβ signaling because TGFβ has been shown to increase stromal and osteoblastic cell replication before their terminal differentiation (50). However, the action of gremlin appeared to be specific to BMP signaling, and marrow stromal cells from gremlin transgenics displayed normal TGFβ-induced Smad 2 phosphorylation.

Members of the DAN/Cerberus family of BMP antagonists, such as Cerberus and Coco, inhibit BMP as well as Wnt activities, suggesting additional potential mechanisms of action for this group of BMP antagonists (51). Wnt molecules control diverse developmental processes, cell proliferation, and survival, and they are critical for osteoblastic differentiation (52–54). Gremlin overexpression in primary stromal cells caused a reduction in free cytosolic β-catenin levels, and the addition of gremlin to ST-2 cells inhibited the Wnt canonical signaling pathway. However, this effect was shared by the specific BMP antagonist noggin, suggesting that it was due to the BMP antagonism of noggin and gremlin. Although extensive interactions have been reported between BMP and Wnt, the hierarchy of their actions in skeletogenesis is not clear (55, 56). BMP-2 up-regulates the expression of Wnt 1 and 3 and the Wnt receptors Frizzled 1 and 9 in marrow stromal cells (57). Smad 4, a signal transducer of the TGFβ superfamily, interacts with β-catenin, and BMP-4 activates the expression of lymphoid enhancer binding protein 1, a β-catenin coactivator (43, 58). Additionally, Wnt 3A signaling enhances BMP-2 induction of chondrogenesis in pluripotent mesenchymal cells (58). In the present study, we found that marrow stromal cells from transgenic mice overexpressing the BMP antagonist gremlin display an inhibition of the Wnt canonical pathway, suggesting that BMP signaling is required for Wnt 3 activation and regulation of gene expression. The specific mechanism of action of gremlin remains tentative, and BMP-2 rescued only selected effects of gremlin, indicating possible BMP-independent effects.

In conclusion, gremlin inhibits bone formation, causing skeletal architectural changes and severe osteopenia.

Acknowledgments

The authors thank Drs. Zhenjan Du, Robert Weinstein, and Janet Hock for valuable suggestions. The authors thank Ms. Lisa Stadmeyer for technical assistance and Ms. Nancy Wallach and Ms. Kimberly Starr for secretarial assistance.

Received June 18, 2004. Accepted October 25, 2004.

Address all correspondence and requests for reprints to: Ernesto Canalis, M.D., Department of Research, Saint Francis Hospital and Medical Center, 114 Woodland Street, Hartford, Connecticut 06105-1299. E-mail: ecanalis@stfranciscare.org.

This work was supported by Grant AR21707 from the National Institute of Arthritis and Musculoskeletal and Skin Diseases (to E.C.) and fellowship awards from the Arthritis Foundation (to E.G. and R.C.P.).

References

1. **Canalis E, Economides AN, Gazzerro E** 2003 Bone morphogenetic proteins, their antagonists and the skeleton. Endocr Rev 24:218–235
2. **Balemans W, Ebeling M, Patel N, Van Hul E, Olson P, Dioszegi M, Lacza C, Wuyts W, Van Den Ende J, Willems P, Paes-Alves AF, Hill S, Bueno M, Ramos FJ, Tacconi P, Dikkers FG, Stratakis C, Lindpaintner K, Vickery B, Foernzler D, Van Hul W** 2001 Increased bone density in sclerosteosis is due to the deficiency of a novel secreted protein (SOST). Hum Mol Genet 10:537–543
3. **Brunkow ME, Gardner JC, Van Ness J, Paeper BW, Kovacevich BR, Proll S, Skonier JE, Zhao L, Sabo PJ, Fu Y, Alisch RS, Gillett L, Colbert T, Tacconi P, Galas D, Hamersma H, Beighton P, Mulligan J** 2001 Bone dysplasia sclerosteosis results from loss of the SOST gene product, a novel cystine knot-containing protein. Am J Hum Genet 68:577–589
4. **Gong Y, Krakow D, Marcelino J, Wilkin D, Chitavat D, Babul-Himi R, Hodgins L, Cremers CW, Cremers FPM, Brunner HG, Reinker K, Rimoin DL, Cohn DH, Goodman FR, Reardon W, Patten M, Francomano CA, Warman ML** 1999 Heterozygous mutations in the gene encoding noggin affect human joint morphogenesis. Nat Genet 21:302–304
5. **Marcelino J, Sciortino CM, Romero MF, Ulatowski LM, Ballock RT, Economides AN, Eimon PM, Harland RM, Warman ML** 2001 Human disease-causing *NOG* missense mutations: effects on noggin secretion, dimer formation, and bone morphogenetic protein binding. Proc Natl Acad Sci USA 98: 11353–11358
6. **Shafritz AB, Shore EM, Gannon FH, Zasloff MA, Taub R, Muenke M, Kaplan FS** 1996 Overexpression of an osteogenic morphogen in fibrodysplasia ossificans progressiva. N Engl J Med 335:555–561
7. **Pearce JJH, Penny G, Rossant J** 1999 A mouse cerberus/Dan-related gene family. Dev Biol 209:98–110
8. **Piccolo S, Sasai Y, Lu B, De Robertis EM** 1996 Dorsoventral patterning in *Xenopus*: inhibition of ventral signals by direct binding of chordin to BMP-4. Cell 86:589–598
9. **Ray RP, Wharton KA** 2001 Twisted perspective: new insights into extracellular modulation of BMP signaling during development. Cell 104:801–804
10. **Tsuchida K, Arai KY, Kuramoto Y, Yamakawa N, Hasegawa Y, Sugino H** 2000 Identification and characterization of a novel follistatin-like protein as a binding protein for the TGF-β family. J Biol Chem 275:40788–40796
11. **Zimmerman LB, DeJesus-Escobar JM, Harland RM** 1996 The Spemann organizer signal noggin binds and inactivates bone morphogenetic protein 4. Cell 86:599–606
12. **Hsu DR, Economides AN, Wang X, Eimon PM, Harland RM** 1998 The *Xenopus* dorsalizing factor gremlin identifies a novel family of secreted proteins that antagonize BMP activities. Mol Cell 1:673–683
13. **Topol LZ, Bardot B, Zhang Q, Resau J, Huillard E, Marx M, Calothy G, Blair DG** 2000 Biosynthesis, post-translation modification, and functional characterization of drm/gremlin. J Biol Chem 275:8785–8793
14. **Topol LZ, Marx M, Laugier D, Bogdanova NN, Boubnov NV, Clausen PA, Calothy C, Blair DG** 1997 Identification of *drm*, a novel gene whose expression is suppressed in transformed cells and which can inhibit growth of normal but not transformed cells in culture. Mol Cell Biol 17:4801–4810
15. **Khokha MK, Hsu D, Brunet LJ, Dionne MS, Harland RM** 2003 Gremlin is the BMP antagonist required for maintenance of Shh and Fgf signals during limb patterning. Nat Genet 34:303–307
16. **Merino R, Rodriguez-Leon J, Macias D, Ganan Y, Economides AN, Hurle JM** 1999 The BMP antagonist gremlin regulates outgrowth, chondrogenesis and programmed cell death in the developing limb. Development 126:5515–5522
17. **Zuniga A, Haramis AP, McMahon AP, Zeller R** 1999 Signal relay by BMP antagonism controls the SHH/FGF4 feedback loop in vertebrate limb buds. Nature 401:598–602
18. **Pereira RC, Economides AN, Canalis E** 2000 Bone morphogenetic proteins induce gremlin, a protein that limits their activity in osteoblasts. Endocrinology 141:4558–4563
19. **Devlin RD, Du Z, Pereira RCP, Kimble RB, Economides AN, Jorgetti V, Canalis E** 2003 Skeletal overexpression of noggin results in osteopenia and reduced bone formation. Endocrinology 144:1972–1978
20. **Erlebacher A, Derynck R** 1996 Increased expression of TGF-β 2 in osteoblasts results in an osteoporosis-like phenotype. J Cell Biol 132:195–210
21. **Irwin N** 1989 Molecular cloning. In: Sambrook J, Fritsch EF, Maniatis T, eds. Analysis and cloning of eukaryotic genomic DNA. New York: Cold Spring Harbor Laboratory Press; 9.32–9.36
22. **Nagy TR, Prince CW, Li J** 2001 Validation of peripheral dual-energy X-ray absorptiometry for the measurement of bone mineral in intact and excised long bones of rates. J Bone Miner Res 16:1682–1687
23. **Parfitt AM, Drezner MK, Glorieux FH, Kanis JA, Malluche H, Meunier PJ, Ott SM, Recker RR** 1987 Bone histomorphometry: standardization of nomenclature, symbols, and units. Report of the ASBMR Histomorphometry Nomenclature Committee. J Bone Miner Res 2:595–610
24. **Franklin RM, Martin MT** 1980 Staining and histochemistry of undecalcified bone embedded in water-miscible plastic. Stain Technol 5:313–321
25. **Barou O, Laroche N, Palle S, Alexandre C, Lafage-Proust M-H** 1997 Pre-osteoblastic proliferation assessed with BrdU in undecalcified, epon-embedded adult rat trabecular bone. J Histochem Cytochem 45:1189–1195
26. **Turner CH, Owan I, Alvey T, Hulman J, Hock JM** 1998 Recruitment and proliferative responses of osteoblasts after mechanical loading *in vivo* determined using sustained-release bromodeoxyuridine. Bone 22:463–469
27. **Weinstein RS, Jilka RL, Parfitt AM, Manolagas SC** 1998 Inhibition of osteoblastogenesis and promotion of apoptosis of osteoblasts and osteocytes by glucocorticoids. J Clin Invest 102:274–282
28. **Gazzerro E, Du Z, Devlin RD, Rydziel S, Priest L, Economides AN, Canalis E** 2003 Noggin arrests stromal cell differentiation *in vitro*. Bone 32:111–119
29. **Choi SJ, Reddy SV, Devlin RD, Menaa C, Chung H, Boyce BF, Roodman GD**

1999 Identification of human asparaginyl endopeptidase (legumain) as an inhibitor of osteoclast formation and bone resorption. J Biol Chem 274:27747–27753
30. **Persson U, Izumi H, Souchelnytskyi S, Itoh S, Grimsby S, Engstrom U, Heldin CH, Funa K, ten Dijke P** 1980 The L45 loop in type I receptors for TGF-β family members is a critical determinant in specifying Smad isoform activation. FEBS Lett 434:83–87
31. **Young CS, Kitamura M, Hardy S, Kitajewski J** 1998 Wnt-1 induces growth, cytosolic β-catenin, and Tcf/Lef transcriptional activation in Rat-1 fibroblasts. Mol Cell Biol 18:2474–2485
32. **Otsuka E, Yamaguchi A, Hirose S, Hagiwara H** 1999 Characterization of osteoblastic differentiation of stromal cell line ST2 that is induced by ascorbic acid. Am J Physiol 277:C132–C138
33. **Zhao M, Harris SE, Horn D, Geng Z, Nishimura R, Mundy GR, Chen D** 2002 Bone morphogenetic protein receptor signaling is necessary for normal murine postnatal bone formation. J Cell Biol 157:1049–1060
34. **Sciaudone M, Gazzero E, Priest L, Delany AM, Canalis E** 2003 Notch 1 impairs osteoblastic cell differentiation. Endocrinology 144:5631–5639
35. **Devlin RD, Du Z, Buccilli V, Jorgetti V, Canalis E** 2002 Transgenic mice overexpressing insulin-like growth factor binding protein-5 display transiently decreased osteoblastic function and osteopenia. Endocrinology 143:3955–3962
36. **Frenkel B, Caparelli C, Van Auken M, Baran D, Bryan J, Stein JL, Stein GS, Lian JL** 1997 Activity of the osteocalcin promoter in skeletal sites of transgenic mice and during osteoblast differentiation in bone marrow-derived stromal cell cultures: effects of age and sex. Endocrinology 138:2109–2116
37. **Kalajzic Z, Liu P, Kalajzic I, Du Z, Braut A, Mina M, Canalis E, Rowe DW** 2002 Directing the expression of a green fluorescent protein transgene in differentiated osteoblasts: a comparison between rat type I collagen and rat osteocalcin promoters. Bone 31:654–660
38. **Charbon GA, Anderson MF** 1991 Reciprocity not proven in hepatic blood flow. Gastroenterology 100:1483–1484
39. **Gori F, Hofbauer LC, Dunstan CR, Spelsberg TC, Khosla S, Riggs BL** 2000 The expression of osteoprotegerin and RANK ligand and the support of osteoclast formation by stromal-osteoblast lineage cells is developmentally regulated. Endocrinology 141:4768–4776
40. **Abe E, Yamamoto M, Taguchi Y, Lecka-Czernik B, O'Brien CA, Economides AN, Stahl N, Jilka RL, Manolagas SC** 2000 Essential requirement of BMPs-2/4 for both osteoblast and osteoclast formation in murine bone marrow cultures from adult mice: antagonism by noggin. J Bone Miner Res 15:663–673
41. **Ogasawara T, Kawaguchi H, Jinno S, Hoshi K, Itaka K, Takato T, Naka K, Okayama H** 2004 Bone morphogenetic protein 2-induced osteoblast differentiation requires Smad-mediated down-regulation of Cdk6. Mol Cell Biol 24:6560–6568
42. **Kawano Y, Kypta R** 2003 Secreted antagonists of the Wnt signaling pathway. J Cell Sci 116:2627–2634
43. **Kratochwil K, Dull M, Farinas I, Galceran J, Grosschedl R** 1996 Lef1 expression is activated by BMP-4 and regulates inductive tissue interactions in tooth and hair development. Genes Dev 10:1382–1394
44. **Bouxsein ML, Turek TJ, Blake CA, D'Augusta D, Li X, Stevens M, Seeherman HJ, Wozney JM** 2001 Recombinant human bone morphogenetic protein-2 accelerates healing in a rabbit ulnar osteotomy model. J Bone Joint Surg Am 83-A:1219–1230
45. **Kloen P, Di Paola M, Borens O, Richmond J, Perino G, Helfet DL, Goumans MJ** 2003 BMP signaling components are expressed in human fracture callus. Bone 33:362–371
46. **Eimon PM, Harland RM** 1999 In *Xenopus* embryos, BMP heterodimers are not required for mesoderm induction, but BMP activity is necessary for dorsal/ventral patterning. Dev Biol 216:29–40
47. **Luo G, Hofmann C, Bronckers AL, Sohocki M, Bradley A, Karsenty G** 1995 BMP-7 is an inducer of nephrogenesis, and is also required for eye development and skeletal patterning. Genes Dev 9:2808–2820
48. **Park J, Ries J, Gelse K, Kloss F, von der MK, Wiltfang J, Neukam FW, Schneider H** 2003 Bone regeneration in critical size defects by cell-mediated BMP-2 gene transfer: a comparison of adenoviral vectors and liposomes. Gene Ther 10:1089–1098
49. **Varghese S, Canalis E** 1997 Regulation of collagenase-3 by bone morphogenetic protein-2 in bone cell cultures. Endocrinology 138:1035–1040
50. **Canalis E, Pash J, Varghese S** 1993 Skeletal growth factors. Crit Rev Eukaryot Gene Expr 3:155–166
51. **Bell E, Munoz-Sanjuan I, Altmann CR, Vonica A, Brivanlou AH** 2003 Cell fate specification and competence by Coco, a maternal BMP, TGF β and Wnt inhibitor. Development 130:1381–1389
52. **Patel MS, Karsenty G** 2002 Regulation of bone formation and vision by LRP5. N Engl J Med 346:1572–1574
53. **Van Wesenbeeck L, Cleiren E, Gram J, Beals RK, Benichou O, Scopelliti D, Key L, Renton T, Bartels C, Gong Y, Warman ML, De Vernejoul MC, Bollerslev J, Van Hul W** 2003 Six novel missense mutations in the LDL receptor-related protein 5 (LRP5) gene in different conditions with an increased bone density. Am J Hum Genet 72:763–771
54. **Bodine PVN, Zhao W, Kharode YP, Bex FJ, Lambert A-J, Goad MB, Gaur T, Stein GS, Lian JB, Komm BS** 2004 The Wnt antagonist secreted frizzled-related protein-1 is a negative regulator of trabecular bone formation in adult mice. Mol Endocrinol 18:1222–1237
55. **Nishita M, Hashimoto MK, Ogata S, Laurent MN, Ueno N, Shibuya H, Cho KWY** 2000 Interaction between Wnt and TGF-β signalling pathways during formation of Spemann's organizer. Nature 403:781–784
56. **Soshnikova N, Zechner D, Huelsken J, Mishina Y, Behringer RR, Taketo MM, Crenshaw III EB, Birchmeier W** 2003 Genetic interaction between Wnt/β-catenin and BMP receptor signaling during formation of the AER and the dorsal-ventral axis in the limb. Genes Dev 17:1963–1968
57. **Rawadi G, Vayssiere B, Dunn F, Baron R, Roman-Roman S** 2003 BMP-2 controls alkaline phosphates expression and osteoblast mineralization by a Wnt autocrine loop. J Bone Miner Res 18:1842–1853
58. **Fischer L, Boland G, Tuan RS** 2002 Wnt signaling during BMP-2 stimulation of mesenchymal chondrogenesis. J Cell Biol 84:816–831

***Endocrinology* is published monthly by The Endocrine Society (http://www.endo-society.org), the foremost professional society serving the endocrine community.**